Cooper, S., and C. E. Helmstetter, "Chomosome Replication and the Division Cycle of *Escherichia coli* B/r," *J. Molecular Biol.*, **31**, 519 (1968).
Donachie, W. D., "Relationships Between Cell Size and Time of Initiation of DNA Replication," *Nature*, **219**, 1077 (1968).
Donachie, W. D., and M. Masters, "Temporal Control of Gene Expression in Bacteria," *The Cell Cycle*, G. L. Whitson and I. L. Cameron, eds., Academic Press, New York (1969).
Fredrickson, A. G., D. Ramkrishna, and H. M. Tsuchiya, "Statistics and Dynamics of Procaryotic Cell Populations," *Math. Biosci.*, **1**, 327 (1967).
Helmstetter, C. E., and S. Cooper, "DNA Synthesis During the Division Cycle of Rapidly Growing *Escherichia coli* B/r," *J. Molecular Biol.*, **31**, 507 (1968).
Herbert, D., "The Chemical Composition of Micro-Organisms as a Function of Their Environment," *Symp. Soc. Gen. Microbiol.*, **11**, 391 (1961).
Maaløe, O., "The Nucleic Acids and the Control of Bacterial Growth," *Symp. Soc. Gen. Microbiol.*, **10**, 272 (1960).
Margolis, S. G., and S. Cooper, "Simulation of Bacterial Growth, Cell Division, and DNA Synthesis," *Comput. Biomed. Res.*, **4**, 427 (1971).
Monod, J., "The Growth of Bacterial Cultures," *Ann. Rev. Microbiol.*, **3**, 371 (1949).
Nishimura, Y., and J. E. Bailey, "On the Dynamics of Cooper-Helmstetter-Donachie Procaryote Populations," *Math. Biosci.*, **51**, 305 (1980).
Prichard, R. H., P. T. Barth, and J. Collins, "Control of DNA Synthesis in Bacteria," *Symp. Soc. Gen. Microbiol.*, **19**, 263 (1969).
Ramkrishna, D., "Statistical Models of Cell Populations," *Advance in Biochemical Engineering 11*, T. K. Ghose, A. Fiechter, and N. Blakebrough, eds., Springer-Verlag, Berlin (1979).
Schaechter, M., O. Maaløe, and N. O. Kjeldgaard, "Dependency on Medium and Temperature of Cell Size and Chemical Composition During Balanced Growth of *Salmonella typhimurium*," *J. Gen. Microbiol.*, **19**, 592 (1958).
Shuler, M. L., S. Leung, and C. C. Dick, "A Mathematical Model for the Growth of A Single Bacterial Cell," *Annals N.Y. Acad. Sci.*, **326**, 35 (1979).

Manuscript received January 14, 1980; revision received May 2, and accepted May 12, 1980.

Effective Diffusivity by The Gas Chromatography Technique: Analysis and Application to Measurements of Diffusion of Various Hydrocarbons in Zeolite NaY

The gas chromatography technique was applied to measurements of diffusion of n-butane in zeolite NaY. The linear chromatography theory failed to explain these results quantitatively, and a significant system nonlinearity was demonstrated. This nonlinearity is likely associated with non-Fickian diffusion. Order of magnitude estimates of the diffusivity could still be obtained, however. Over the range of temperatures 105 to 240°C, the n-butane diffusivities were in the range 10^{-8} to 10^{-6} cm^2/s. Similar results were obtained with n-hexane and calculated diffusivities were about an order of magnitude smaller than the corresponding n-butane values. In contrast, limited experiments with cyclohexane, 2, 2-dimethylbutane, and *trans*-decalin were entirely consistent with the linear chromatography theory. At the measurement temperatures, the intracrystalline diffusion was too rapid to be detected in any of these systems. Attempts to operate at lower temperatures where diffusion might be significant were frustrated by extensive peak broadening and concomitant loss of detector response.

L.-K. P. HSU
and
H. W. HAYNES, JR.
Chemical Engineering Department
University of Mississippi
University, MS 38677

SCOPE

Large pore zeolites and in particular the faujasite-type zeolites (zeolites *X* and *Y*) have seen widespread applications as cracking and isomerization catalysts (Haynes, 1978). In spite of this, information concerning mass transfer in the large pore zeolites is only fragmentary. When studying the information that is available, one frequently observes discrepancies of several orders of magnitude in the diffusivities reported by different investigators employing different techniques of measurement. Many times these discrepancies arise from failure of the system equations to properly describe all important physical phenomena. This can go unrecognized if no attempt is made to compare the model predictions with the experiment.

One of the more popular methods for evaluating effective diffusivities in heterogeneous catalysts is based on gas chromatography. In earlier work from our laboratory, the GC-technique was successfully employed to evaluate diffusivities in small pore zeolites (Sarma and Haynes, 1974a) and these results were confirmed by independent investigators using an adsorption rate technique (Shah and Ruthven, 1977).

One objective of the present investigation was to apply the GC-technique to measurements of diffusion of various hydrocarbons in large pore zeolites. A necessary prerequisite was to provide a rigorous test of the linear chromatography theory in its ability to describe the experimental results.

Several important improvements were incorporated into the data analysis procedure to provide the most meaningful com-

Correspondence concerning this paper should be addressed to H. W. Haynes, Jr.

0001-1541-81-4216-0081-$2.00.

parison possible between theory and experiment. First, a general form of the linear chromatography theory was developed for application to a distribution of crystallite sizes. Second, a novel means of accounting for axial dispersion was used which does not require dumping and repacking the bed. Neither does it require an assumed form for the velocity dependence of the axial dispersion coefficient. Finally, we utilized an improved method for extracting the model parameters from the experimental data. This method is based on the frequency domain analysis of Hays, et al. (1967) coupled with numerical integrations by Filon's method. This is a general method of analysis and its advantages can be realized in any stimulus-response testing experiment.

CONCLUSIONS AND SIGNIFICANCE

Extensive tests on the n-butane/NaY system revealed a velocity dependence of the calculated intracrystalline diffusivity and a failure of the linear chromatography theory to fit the experimental results precisely. Variation of the inlet pulse size was shown to have an effect on the n-butane response curves, thus, demonstrating a system nonlinearity. The effect of pulse size was diminished at the smallest pulse sizes investigated indicating that the system was approaching linearity. However, there was a lower limit on pulse size below which the detector signal became obscured by background noise.

Despite these problems with the n-butane/NaY system, intracrystalline diffusion was clearly affecting the results, and order of magnitude estimates of the diffusivities could be obtained. Over the range of temperatures studied, 105 to 240°C, the intracrystalline diffusivities were of the order of 10^{-8} to 10^{-6} cm^2/s. These estimates were obtained from calculations based on the complete distribution of crystallite sizes. Calculations based on the mean crystallite diameter yielded much smaller diffusivities (by almost two orders of magnitude). This may explain in part the wide disparities between zeolite diffusivities reported in the literature.

Limited experiments with other hydrocarbons (n-hexane, 2,2-dimethylbutane, cyclohexane and *trans*-decalin) were conducted with the same NaY zeolite. The n-hexane results were similar to the results obtained with n-butane; only the calculated diffusivities were about an order of magnitude smaller. In contrast to the n-butane results, the response curves for the 2,2-dimethylbutane, cyclohexane and *trans*-decalin experiments were all well described by the linear chromatography theory. Intracrystalline diffusion was too rapid to be observed in these systems at the temperatures studied (280°C for dimethylbutane, 202-280°C for cyclohexane and 280°C for *trans*-decalin). The extensive sorption, characteristic of experiments with high molecular weight hydrocarbons, dispersed the pulse to such an extent that the limit on detector sensitivity was exceeded. For example, the *trans*-decalin pulse was eluted over a period of time in excess of 11 hours and the response peak was just barely detectable.

We can only speculate on the cause of the observed nonlinearities in some of our experiments. Since nonlinear behavior was only observed during experiments in which intracrystalline diffusion was significant, we are inclined to accept the concentration dependent diffusivity explanation. This conclusion is supported by Ruthven's (1977) observation that even in the Henry's law region Fickian diffusivities of small molecular species diffusing in large pore zeolites are approximately inversely proportional to concentration.

It appears, therefore, that the application of the gas chromatography technique to measurements of intracrystalline diffusion in zeolites is subject to serious limitations. The adsorption of high molecular weight or strongly sorbed species gives rise to such extensive peak broadening that limits on detector sensitivity may be exceeded. This imposes a practical lower limit on the temperature of measurement. On the other hand, measurements of diffusion of small, low molecular weight species in large pore zeolites are complicated by nonlinearities most likely associated with non-Fickian diffusion.

The frequency domain analysis of Hay's et al. (1967), coupled with numerical integrations by Filon's method provides a powerful means of extracting parameter values from gas chromatography pulse dispersion experiments. Once the optimum parameter values are obtained, the theoretical and experimental residence time distributions should be compared in the time domain to test goodness of fit. The procedures utilized in the present investigation are recommended for general application to pulse testing experiments.

Gas chromatography has seen widespread application to measurements of effective diffusivity in heterogeneous catalysts, and models with varying degrees of complexity have been compared to the experimental results by a variety of techniques. The most comprehensive models that have been employed thus far include terms to account for axial dispersion, external mass transfer, intraparticle diffusion in both macropore and micropore regions of the pellet, and a finite rate of adsorption (Haynes and Sarma, 1973; Hashimoto and Smith, 1973).

An analysis based on the moments of the chromatogram (or equivalently the HETP analysis) has been the most popular method of extracting model parameters from the experimental response curves. However, this method suffers from the practical limitation that the evaluation of third and higher moments requires experimental data of a precision that is not usually attained in the laboratory. Consequently, the investigator does not have a sufficient number of equations to conveniently deal with multi-parameter systems. Furthermore, much information is lost when the response curve is reduced to two simple statistics. For example, the degree of skewness which is very important to measurements of diffusion (Haynes, 1975) is not reflected in the first two moments. Finally, an evaluation of the model parameters using the moments analysis does not provide a check on the accuracy with which the model represents the actual response curve.

This report first presents the linear chromatography model in a very general form that contains an important feature absent in previous versions; namely, the ability to handle a distribution of crystallite sizes. We then show how the model parameters can be conveniently extracted from the experimental response curves using a Fourier transform technique (Hays et al., 1967) coupled with integrations by Filon's (Tranter, 1971) method. This method of analysis does not appear to have been used previously in the analysis of GC pulse dispersion data. We conclude by applying the model and analysis technique to experimental measurements of hydrocarbon diffusion in zeolite NaY.

THE MODEL

The model developed in an earlier communication (Haynes and Sarma, 1973) has been modified for use in the present study.

In the original development, it was assumed that both a gas phase and an adsorbed phase existed in the microparticles. However, most investigators of diffusion in zeolites have based their analysis on a model of single-phase sorption in the zeolite crystal, since molecular species sorbed in zeolites are never free from force fields associated with the pore wall.

Accordingly, the intracrystalline mass balance is given by Eq. 1 where q = moles adsorbate/cc crystal. In the boundary condition, Eq. 2, provision is made for a finite rate of adsorption. The zeolite crystallite size distribution is taken into account in Eq. 5 where $p(R_x)dR_x$ is the number of particles with radii between R_x and $R_x + dR_x$. Finally, to test for the significance of macropore adsorption, a macropore adsorption equilibrium constant, K_y, was included in the macroparticle mass balance, Eq. 4. The model equations are summarized in Eqs. 1 to 12.

$$\mathscr{D}_c\left(\frac{\partial^2 q}{\partial x^2}+\frac{2}{x}\frac{\partial q}{\partial x}\right)=\frac{\partial q}{\partial t} \tag{1}$$

$$\frac{\partial q}{\partial x}(R_x,\,t)=\frac{k_a}{\mathscr{D}_c}\left[C_y(y,\,t)-\frac{1}{K_c}\,q(R_x,\,t)\right] \tag{2}$$

$$\frac{\partial q}{\partial x}(0,\,t)=0 \tag{3}$$

$$\mathscr{D}_y\left(\frac{\partial^2 C_y}{\partial y^2}+\frac{2}{y}\frac{\partial C_y}{\partial y}\right)+\mathscr{W}_x\,(1-\theta_y)=\theta_y\,(1+K_y)\frac{\partial C_y}{\partial t} \tag{4}$$

$$\mathscr{W}_x=-\frac{3\mathscr{D}_c}{\overline{R_x^3}}\int_0^\infty R_x^2\frac{\partial q}{\partial x}(R_x,\,t)\,p(R_x)dR_x \tag{5}$$

$$\frac{\partial C_y}{\partial y}(0,\,t)=0 \tag{6}$$

$$\frac{\partial C_y}{\partial y}(R_y,\,t)=\frac{k_f}{\mathscr{D}_y}\left[C_z(z,\,t)-C_y(R_y,\,t)\right] \tag{7}$$

$$\mathscr{D}_z\frac{\partial^2 C_z}{\partial z^2}-v\frac{\partial C_z}{\partial z}+\mathscr{W}_y\,(1-\theta_z)=\theta_z\frac{\partial C_z}{\partial t} \tag{8}$$

$$\mathscr{W}_y=-\frac{3\mathscr{D}_y}{R_y}\frac{\partial C_y}{\partial y}(R_y,\,t) \tag{9}$$

$$C_z(0,\,t)=\delta(t) \tag{10}$$

$$C_z(\infty,\,t)=\text{finite} \tag{11}$$

$$q(x,\,0)=C_y(y,\,0)=C_z(z,\,0)=0 \tag{12}$$

From these equations, we can derive an expression for the exiting concentration, $C_z(L,\,s)=\tilde{E}(s)$, in the Laplace domain. Thus:

$$\tilde{E}(s)=\exp\left[-\frac{vL}{2\mathscr{D}_z}\left(\sqrt{1+\frac{4\gamma\mathscr{D}_z}{v}}-1\right)\right] \tag{13}$$

where

$$\gamma=\frac{\theta z}{v}\,s+\frac{3(1-\theta_z)k_f}{vR_y}\left(\frac{\beta R_y\coth\beta R_y-1}{\frac{k_f R_y}{\mathscr{D}_y}+\beta R_y\coth\beta R_y-1}\right) \tag{14}$$

$$\beta^2=\frac{\theta_y(1+K_y)}{\mathscr{D}_y}\,s+\frac{(1-\theta_y)}{\mathscr{D}_y}\left(-\frac{\tilde{\mathscr{W}}_x}{\tilde{C}_y}\right) \tag{15}$$

$$\alpha^2=s/\mathscr{D}_c \tag{16}$$

and

$$-\frac{\tilde{\mathscr{W}}_x}{\tilde{C}_y}=\frac{3\mathscr{D}_c}{\overline{R_x^3}}\int_0^\infty R_x\left(\frac{\alpha R_x\coth\alpha R_x-1}{\frac{\mathscr{D}_c}{k_a R_x}(\alpha R_x\coth\alpha R_x-1)+\frac{1}{K_c}}\right)p(R_x)dR_x \tag{17}$$

Often the experimental conditions can be adjusted to eliminate contributions from macropore adsorption and diffusion, external mass transfer, and finite rates of adsorption. With these simplifications, i.e. in the limit as $\mathscr{D}_y\to\infty$, $k_f\to\infty$, $k_a\to\infty$ and $K_y\to 0$, Eqs. 14 through 17 become:

$$\gamma=\frac{\theta_z}{v}\,s+\frac{(1-\theta_z)\theta_y}{v}\,s+\frac{(1-\theta_z)\,(1-\theta_y)K_c}{v}\left(-\frac{\tilde{\mathscr{W}}_x}{\tilde{C}_y}\right) \tag{18}$$

where

$$-\frac{\tilde{\mathscr{W}}_x}{\tilde{C}_y}=\frac{3\mathscr{D}_c K_c}{\overline{R_x^3}}\int_0^\infty R_x\,(\alpha R_x\coth\alpha R_x-1)\,p(R_x)dR_x \tag{19}$$

Frequently, the crystallite size distribution is well described by a log-normal distribution for which:

where $$p(R_x)=\frac{1}{\sqrt{2\pi\sigma^2}\,R_x}\exp\left[-\frac{(\ln R_x-\mu)^2}{2\sigma^2}\right] \tag{20}$$

Upon making the substitution:

$$R_x=\exp\left(\mu+\sqrt{2\sigma^2}\,z\right) \tag{21}$$

and combining with Eq. 19, we obtain:

$$-\frac{\tilde{\mathscr{W}}_x}{\tilde{C}_y}=\frac{3\mathscr{D}_c K_c}{\sqrt{\pi}\,\overline{R_x^3}}\int_{-\infty}^\infty e^{-z^2}\,R_x\,(\alpha R_x\coth\alpha R_x-1)\,dz \tag{22}$$

The integral of Eq. 22 is of a form which can be rapidly evaluated by the Gauss-Hermite quadrature formula (Scheid, 1968).

On the other hand, if the crystallite size can be assumed constant, we have $p(R_x)=\delta(R_x)$ and Eq. 18 simplifies to:

$$\gamma=\frac{\theta_z}{v}\,s+\frac{\theta_z\,(1-\theta_y)}{v}\,s+\frac{3\,(1-\theta_z)\,(1-\theta_y)\,\mathscr{D}_c K_c}{vR_x^2}\,(\alpha R_x\coth\alpha R_x-1) \tag{23}$$

Eqs. 13 and 23 are identical to the result obtained earlier (Haynes and Sarma, 1973), if we make the substitutions: $K_c=\theta_x\,(1+K_a)$ and $\mathscr{D}_c=\mathscr{D}_x/\theta_x\,(1+K_a)$. Here, θ_x is the micropore porosity and $\mathscr{D}_x$ and K_a are the microparticle diffusivity and adsorption constant respectively in the two-phase sorption model. Previously, Shah and Ruthven (1977) showed that the two sorption models gave mathematically equivalent results, when these substitutions were made.

METHOD OF ANALYSIS

Consider a system being subjected to an arbitrary pulse input, $X(t)$, with response $Y(t)$. These curves can be transformed into the frequency domain by applying the definition of the Fourier transform. Thus:

$$\tilde{X}(j\omega)=Re_x\,(\omega)+jIm_x\,(\omega) \tag{24}$$

where

$$Re_x(\omega)=\int_0^\infty X(t)\cos\omega t\,dt \tag{25}$$

$$Im_x(\omega)=\int_0^\infty X(t)\sin\omega t\,dt \tag{26}$$

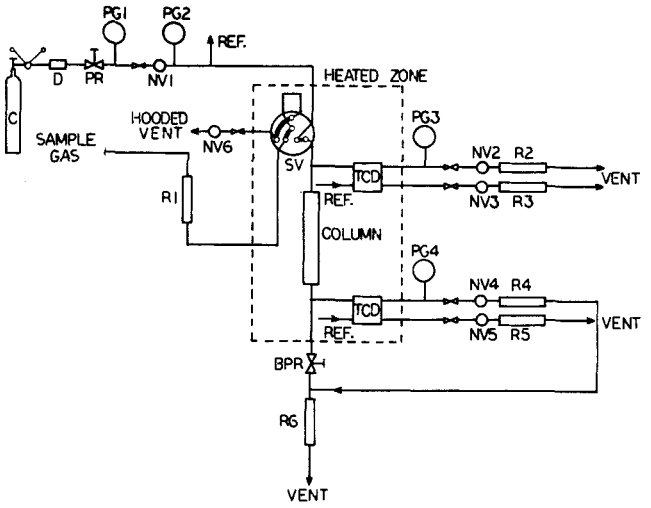

Figure 1. Gas chromatography diffusivity apparatus (*BPR* = Back Pressure Regulator, *NV* = Fine Needle Valve, *PG* = Pressure Gauge, *PR* = Pressure Regulator, *R* = Rotameter, *SV* = 6-port Sample Valve, *TCD* = Thermal Conductivity Detector).

and analogous equations are written for $\tilde{Y}(j\omega)$. The transformed E-curve is obtained by complex division:

$$\tilde{E}(j\omega) = \tilde{Y}(j\omega)/\tilde{X}(j\omega) \tag{27}$$

Transformation into the frequency domain then requires numerical evaluation of integrals of the type given by Eqs. 25 and 26. Problems are encountered when standard numerical techniques are applied to these integrals at high values of frequency, ω, due to the rapidly oscillating integrand. We have tried several integration methods and found a technique due to Filon (Tranter, 1971) to provide excellent results, far superior to any of the others. The Fast Fourier Transform gives good results, but it is unsuitable for manual extraction of data from a strip chart due to restrictions on the number of points that must be read from the curve.

As discussed by Hays, et al. (1967), an objective function in the frequency domain mathematically equivalent to a least squares criterion in the time domain is given by:

$$\phi' = \frac{1}{\pi}\int_0^\infty ([Re(\omega) - Re_c(\omega)]^2 + [Im(\omega) - Im_c(\omega)]^2)\, d\omega \tag{28}$$

where $Re(\omega)$ and $Im(\omega)$ are the real and imaginary parts of the experimental E-curve transformed into the frequency domain, Eq. 27, and $Re_c(\omega)$ and $Im_c(\omega)$ are calculated values obtained by substituting $s = j\omega$ into Eq. 13. The problem is now to find values of the model parameters contained in Re_c and Im_c which minimize ϕ'. We have had good success using a Taylor series linearization procedure to solve the optimization problem.

First, we approximate the integral of Eq. 28 by a finite sum giving a slightly modified objective function:

$$\phi = \sum_{i=1}^{n} (Re_i - Re_{c,i})^2 + (Im_i - Im_{c,i})^2 \tag{29}$$

where $Re_i = Re(\omega_i)$, etc. This is equivalent to the trapezoid rule approximation (less end corrections), when the ω_i are equally spaced. Now assume that we have initial guesses of the m-model parameters, $b_k^{(0)}$, $k = 1, 2 \ldots m$. Then, for any value of ω_i, we can approximate Re_c and Im_c at an improved set of parameter values, b_k, by a Taylor series truncated after the first derivative. The Taylor series approximations are substituted into the sum of Eq. 29, and a linear set of algebraic equations corresponding to the objective function minimum is obtained by setting the derivatives $\partial\phi/\partial\Delta b_k = 0$ for each parameter. The algebraic equations are solved for the Δb_k and the computation is repeated with the revised $b_k^{(0)}$ until the b_k differ from the $b_k^{(0)}$ by a small predetermined error deemed acceptable.

Once the optimum parameter values are determined, the corresponding time domain solution can be calculated from:

$$E_c(t) = \frac{1}{\pi}\int_0^\infty [Re_c(\omega)\cos\omega t - Im_c(\omega)\sin\omega t]\, d\omega \tag{30}$$

This equation can be derived from the complex inversion integral of Laplace transforms as outlined previously (Haynes, 1975), or it can be obtained by applying Euler's identity to the exponential in the inverse Fourier transform. In practice, the time domain solution is obtained by applying Filon's integration method to each of the integrals in Eq. 31:

$$E_c(t) = \frac{1}{\pi}\int_0^{\omega\max} Re_c(\omega)\cos\omega t\, d\omega - \frac{1}{\pi}\int_0^{\omega\max} Im_c(\omega)\sin\omega t\, d\omega + \text{Error Term} \tag{31}$$

The upper limit, ω_{max}, is an arbitrary value chosen sufficiently large to insure disappearance of the integrand. Eq. 31 can also be utilized for calculating the "experimental" E-curve from the recorded input and output curves. In this case, $Re_c(\omega)$ and $Im_c(\omega)$ are replaced with experimental values, $Re(\omega)$ and $Im(\omega)$, derived from Eq. 27.

EXPERIMENTAL PROCEDURE

A schematic of the apparatus is provided in Figure 1. The flow of carrier gas, helium, is regulated by needle valve NV1 and passes successively through a sample injection device, and inlet splitting tee, the column, an outlet splitting tee, and a back pressure regulator, BPR. The column pressure was controlled at 34 kPa (5 psig) and the pressure drop was always less than 6.89 kPa (1 psi). The input and output pulses are recorded by thermal conductivity detectors (TCD), Gow Mac Model 10-952. The version of the apparatus, Figure 1, employs a six-port sampling valve, Valco Model VSV-6-HTa for sample injection. The sample loop volume is either 0.56 (runs HSU07-HSU14) or 2.79 cc (runs HSU15-HSU17). In an alternative configuration the sample is introduced by syringe through a heated injection port, and a small tube of silica gel [6.35 mm (0.25 in.) O.D. × 101.6 mm (4 in.) length] is placed between the injection port and the inlet splitting tee to enhance the dispersion of the inlet pulse.

The column, sample injection device, and detectors are contained in a forced air oven. Heat is provided by electrical resistance heaters distributed along each of the four walls (sides) of the oven. Baffles are located between the heating elements and the usable zone of the oven, and air is circulated from bottom to top between the baffles and the wall by a squirrel cage blower at the bottom. Air returns to the blower through the central (usable) zone of the oven. This arrangement makes possible isothermal operation to within the sensitivity of the digital temperature readout meters (1°C).

The zeolite sample employed in these studies was purchased from the Linde Div. of Union Carbide and carries the designation LZ-Y52. Analysis of the original zeolite powder indicated that the sodium-aluminum ratio was nonstoichiometric, and so attempts were made to prepare a stoichiometric zeolite by subjecting the sample to ion exchanges with a 1 M sodium acetate solution. This procedure was only partially successful since the Na/Al ratio of the treated sample was 0.93 by analysis. A comparison of the untreated and treated samples by X-ray analysis indicated no loss of crystallinity.

The sodium-exchanged samples were pilled without binder, dried, crushed, and sieved to the desired mesh size. Mercury porosimetry analysis of the pilled samples revealed a substantial macropore volume in the neighborhood of 2000 Å pore radius (Hsu, 1979). The zeolite powder was subjected to a video-microscopy particle size analysis at the Pittsburgh Energy Technology Center of the U.S. D.O.E. under the direction of M. P. Mathur. The particle-size distribution was found to be log-normal (Eq. 20) with $\mu = -8.428$ and $\sigma = 0.8520$ (for R_x in cm). Details are available in Hsu (1979).

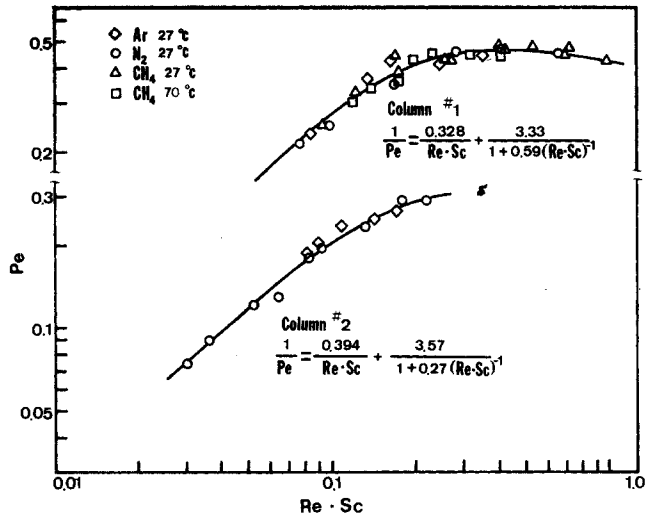

Figure 2. Axial dispersion correlations for Column 1 and Column 2.

Correction for Axial Dispersion

Generally, axial dispersion cannot be avoided in measurements of effective diffusivity by the gas chromatography technique. Sarma and Haynes (1974b), for example, observed that axial dispersion was responsible for as much as 75% of the observed variance in their studies of helium diffusion in six commercial amorphous catalysts. Two methods have been used to account for the axial dispersion effect.

Smith and Hashimoto (1973) assume that the axial dispersion coefficient varies with velocity according to $\mathscr{D}_z = \alpha + \beta v$; and thereby isolate the term containing the diffusivity in a regression equation relating the variance of the chromatogram to the carrier gas velocity. This method avoids the necessity for dumping and repacking the bed. However, Hsiang and Haynes (1977) found that the velocity dependence of the axial dispersion coefficient was more in accord with $\mathscr{D}_z = \alpha + \beta v^n$, where the exponent n, could take on values between one and two. While the errors involved in dumping and repacking the bed were statistically significant, they were deemed acceptable for most applications. Previous studies in our laboratory relied on "blank" experiments with nonporous particles similar in size and shape to the sample catalyst for obtaining values of the axial dispersion coefficient.

Neither of these methods is entirely acceptable from the standpoints of preciseness and convenience. Accordingly, we are employing a novel procedure for evaluating the axial dispersion term in these studies of intracrystalline diffusion in large pore zeolites. This new approach is based on the fact that in the limit of infinite diffusive transport, only the axial dispersion term contributes to the broadening of the response pulse (Haynes and Sarma, 1973; Haynes, 1975). The macropore diffusion term is eliminated by grinding the catalyst to a fine particle size. The micropore diffusion term is eliminated by conducting experiments with small diameter molecules, e.g. N_2 (3.0 Å), Ar (3.84 Å) and CH_4 (4.0 Å), which diffuse rapidly in the large-pore faujasite structure.

Thus, the axial dispersion term for N_2, Ar, and CH_4 in the catalyst bed is evaluated from pulse dispersion experiments on the same bed of catalyst that is to be subjected to the hydrocarbon pulses. From a

TABLE 1. COLUMN DETAILS

	Column No. 1	Column No. 2	Column No. 3
Length, cm	30.5	30.5	30.5
Inside Diameter, cm	1.080	0.781	0.781
Bed Porosity	0.430	0.438	0.401
Particle Mesh Size	20/30	40/60	40/50
Avg. Particle Diameter, mm	0.715	0.335	0.359

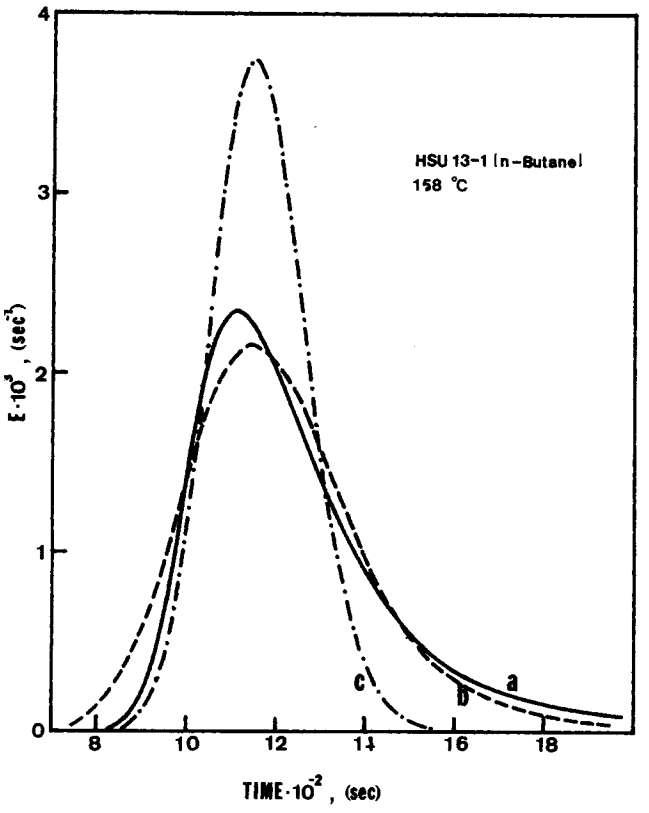

Figure 3. Comparison of experimental and calculated response curves for n-butane diffusion in zeolite NaY at 158°C, 2.25 cm/s: a = experimental; b = calculated ($\mathscr{D}_c = 0.743 \times 10^{-7}$ cm²/s, $K_c = 297$); c = calculated ($\mathscr{D}_c = \infty$, $K_c = 288$).

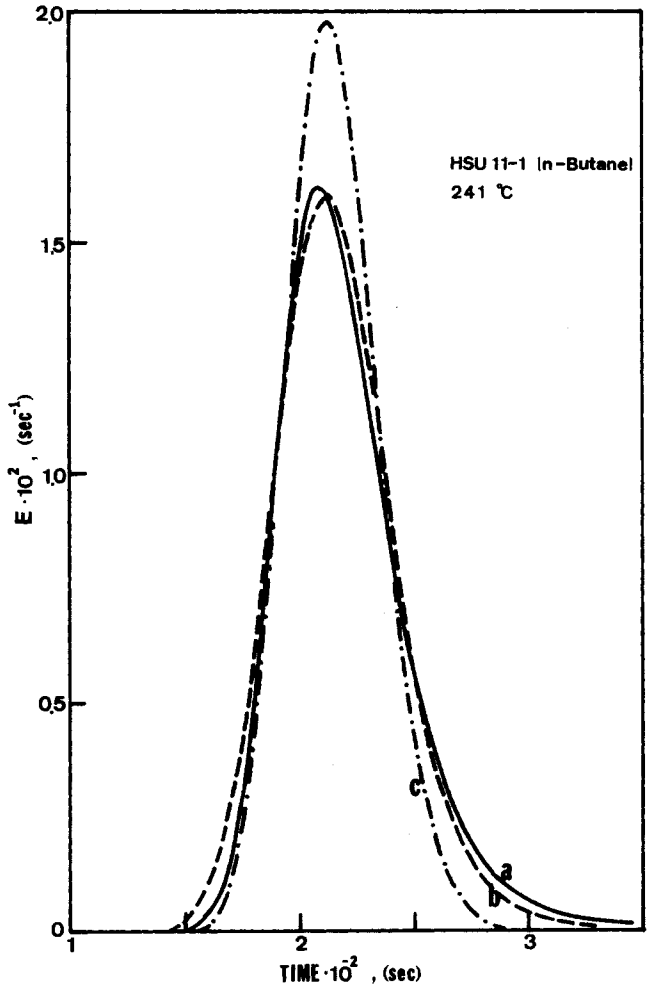

Figure 4. Comparison of experimental and calculated response curves for n-butane diffusion in zeolite NaY at 241°C, 2.57 cm/s: a = experimental; b = calculated ($\mathscr{D}_c = 13.6 \times 10^{-7}$ cm²/s, $K_c = 59$); c = calculated ($\mathscr{D}_c = \infty$, $K_c = 58.6$).

TABLE 2. RESULTS FROM FREQUENCY DOMAIN ANALYSIS OF n-BUTANE RESULTS (ADJUSTABLE PARAMETERS: K_c, $\mathcal{D}_c$)

Run No.	$\bar{d}p$ (mm)	T (°C)	v (cm/s)	$\mathcal{D}_z$ (cm²/s)	K_c	$\mathcal{D}_c \times 10^7$ (cm²/s)	Activation
HSU07-3	0.715	178	4.37	0.699	183	6.02	A
HSU07-4	0.715	178	5.88	0.987	184	6.58	A
HSU07-5	0.715	178	5.38	0.889	195	7.23	A
HSU08-1	0.715	242	3.20	0.496	59.0	25.4	A
HSU08-3	0.715	242	4.54	0.712	60.5	32.4	A
HSU08-4	0.715	242	6.87	1.141	61.4	44.8	A
HSU08-5	0.715	242	9.01	1.572	61.4	58.8	A
HSU09-3	0.335	180	3.17	0.362	189	2.29	B
HSU09-4	0.335	180	2.74	0.328	186	2.02	B
HSU09-5	0.335	180	2.42	0.304	182	1.95	B
HSU10-1	0.335	199	2.37	0.309	121	4.04	B
HSU10-2	0.335	199	2.15	0.294	126	3.86	B
HSU10-3	0.335	199	2.15	0.294	124	3.71	B
HSU10-4	0.335	199	2.84	0.362	123	4.51	B
HSU11-1	0.335	241	2.57	0.345	59.0	13.6	B
HSU11-3	0.335	241	2.17	0.319	59.5	12.0	B
HSU11-4	0.335	241	1.79	0.297	59.0	10.8	B
HSU12-1	0.715	199	3.75	0.585	119	11.1	A
HSU12-3	0.715	199	4.96	0.799	121	13.3	A
HSU12-4	0.715	199	6.40	1.076	121	17.5	A
HSU12-7	0.715	199	8.53	1.512	123	22.8	A
HSU13-1	0.335	158	2.25	0.283	297	0.743	B
HSU13-2	0.335	158	2.92	0.334	298	0.862	B
HSU13-3	0.335	158	2.64	0.312	286	0.959	B
HSU14-3	0.335	180	2.84	0.336	175	2.50	C
HSU14-4	0.335	180	3.13	0.359	180	2.67	C
HSU15-1	0.335	151	0.516	0.246	251	0.821	D
HSU15-2	0.335	151	0.618	0.248	255	1.08	D
HSU16-1	0.335	124	0.524	0.221	463	0.402	D
HSU16-2	0.335	124	0.839	0.229	491	0.540	D
HSU17-1	0.335	105	0.446	0.205	715	0.239	D
HSU17-2	0.335	105	0.596	0.208	762	0.238	D

A = One 16-h activation at 400°C in flowing helium. Prior to this treatment, the sample was exposed to temperatures of 200°C (≈12 h) and 292°C (≈6 h) in flowing helium.
B = One 16-h activation at 400°C in flowing helium.
C = Treatment B followed by a second 16-h activation at 400°C in flowing helium.
D = Treatment C followed by a third 16-h activation at 400°C in flowing helium.

dimensionless plot of these results, one can calculate the axial dispersion coefficients for other molecular species in the same catalyst bed. Dimensional analysis considerations dictate that the particle Peclet No., $Pe = vd_p/\mathcal{D}_z$, be correlated with particle Reynolds No., $Re = d_p v\rho/\mu$, and Schmidt No., $Sc = \mu/\rho\mathcal{D}_m$, but for gases a correlation of Pe with the product $Re \times Sc$ is adequate (Gunn, 1969; Miyauchi and Kikuchi, 1975). The validity of this approach can be tested in two ways.

First, if the dispersion data for a number of species of differing molecular size fall on a common curve when Pe is plotted vs. $Re \times Sc$, it is unlikely that intracrystalline mass transfer is significant in any of the experiments. (Intracrystalline diffusion in zeolites is a strong function of molecular size, and so is therefore the contribution to the observed variance provided that the diffusion is slow enough to be observed.) A second indication of significant mass transfer resistances is the shape of the chromatogram. As discussed by Haynes (1975) and Chou (1979), a Gaussian response curve is indicative of infinitely rapid particle as*sociated with mass transfer resistances; i.e., the peak broadening is* entirely a consequence of axial dispersion.

RESULTS

Prior to the diffusion experiments, a preliminary study was undertaken to evaluate the magnitude of possible "extracolumn" contributions to the observed response curves (Hsu, 1979). From experiments on different length columns, it was demonstrated that extracolumn contributions to the mean and variance of the response curve could be neglected. It was also shown that the input pulse width was of the order of tenths of a second, when the sample was introduced by means of the sample injection valve. Since the width of the output peak for experiments with adsorbable hydrocarbons was of the order of minutes (or even hours), the assumption of an impulse input is reasonable. (Input pulses introduced by the syringe arrangement were of finite width, however.)

n-Butane Experiments

Two columns were prepared for the n-Butane studies. Details are provided in Table 1 under Column No. 1 and No. 2. These columns were subjected to impulses of N_2, Ar, and CH_4 over a range of velocities and the response curves were fit in the time domain (Hsiang and Haynes, 1977) by adjusting the parameters $\mathcal{D}_z$ and K_c using a nonlinear least squares regression program. These results for $\mathcal{D}_z$ were combined with tabulated molecular transport properties and plotted in Figure 2. For a given column the points all fall on a single curve, and it may be concluded that axial dispersion is responsible for the pulse broadening. Furthermore, the emerging peaks were all nearly symmetrical. Asymptotic values of Pe in this range are consistent with previous studies of axial dispersion in beds of small diameter particles (Edwards and Richardson, 1968; Suzuki and Smith, 1972).

The experiments with n-butane were typically characterized

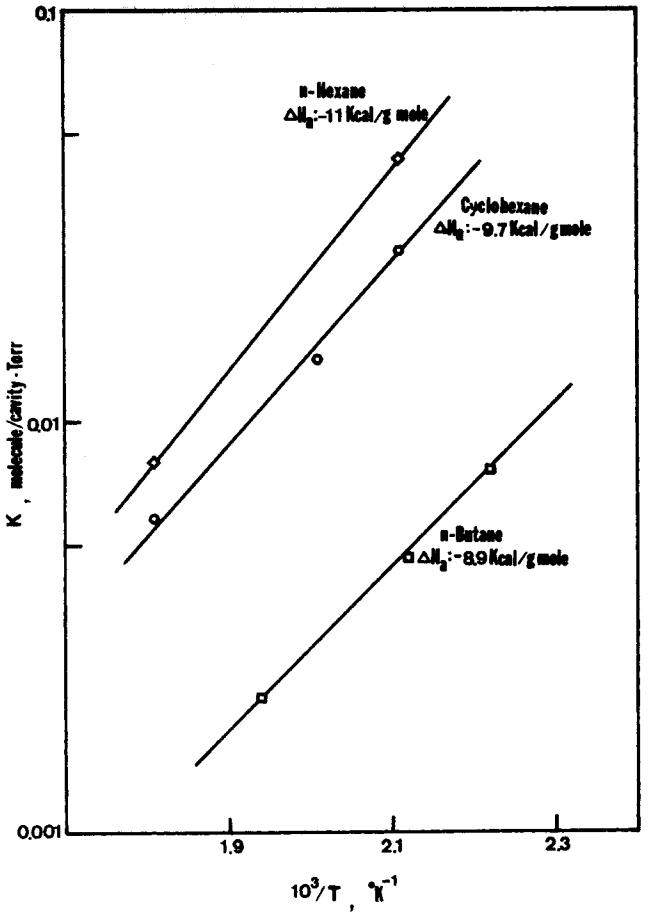

Figure 5. Variation of Henry's law constant with temperature.

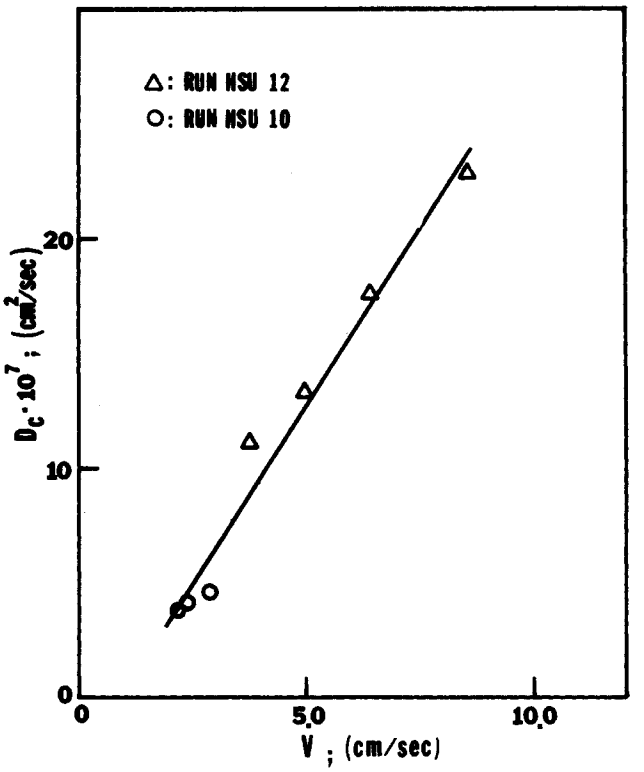

Figure 6. Velocity dependence of calculated diffusivity.

by a skewed response pulse which according to the model is indicative of a finite mass transfer resistance (Haynes, 1975, Chou, 1979). Examples are provided by the solid curves in Figures 3 and 4. The degree of tailing was greatest at lower temperatures. Calculations based on estimated macropore diffusivities (Satterfield, 1970) indicated that macropore contributions to the dispersion could be neglected in these small particles. Contributions from external mass transfer could also be neglected as revealed in calculations based on the mass transfer correlation of Wakao et al. (1979). Details of these computations which involved a comparison of estimated variances are available in Hsu's thesis (1979).

It is difficult to estimate an adsorption rate constant *a priori*, and while some authors claim to have evaluated this parameter from GC pulse dispersion experiments we are skeptical. At least one other group of authors shares this belief (Gangwal et al. 1978). For the moment let us assume that the rate of adsorption is infinitely fast. Then, the version of the model which seems appropriate for analysis of the n-butane diffusion data is given by Eqs. 13, 18, and 22. Each of the n-butane response curves was fit to this simplified model with adjustable parameters K_c and $\mathcal{D}_c$. The axial dispersion coefficients, $\mathcal{D}_z$, were calculated from the correlations of Figure 2. Results of these computations are summarized in Table 2.

Focusing our attention first on the sorption equilibrium constant, K_c, we see a strong temperature effect, but no evidence of any significant particle size or velocity dependence. From the temperature dependence of this constant, the isosteric heat of adsorption is calculated to be 37.3 kJ (−8.9 kcal)/mol, Figure 5. The diffusivity values in Table 2 exhibit a temperature dependence, but also of great concern is the observation of a clear velocity dependence, Figure 6. This, of course, is inconsistent

Table 3. Parameter Sensitivity Analysis on Results on Run Hsu 13-1

Case	ϕ*	$\mathcal{D}_z$ (cm²/s)	K_c	$\mathcal{D}_c \times 10^7$ (cm²/s)	$\mathcal{D}_y$ (cm²/s)	k_f (cm/s)	k_a (cm/s)	Optimization Parameter
(a)	0.45	0.283	297	0.743	∞	∞	∞	K_c, $\mathcal{D}_c$
(b)	0.40	0.226	298	0.645	∞	∞	∞	K_c, $\mathcal{D}_c$
(c)	0.49	0.340	296	0.879	∞	∞	∞	K_c, $\mathcal{D}_c$
(d)	0.16	0.00070	302	0.401	∞	∞	∞	K_c, $\mathcal{D}_c$, $\mathcal{D}_z$
(e)	0.46	0.283	297	0.754	0.080	∞	∞	K_c, $\mathcal{D}_c$, $\mathcal{D}_y$
(f)	0.46	0.283	297	0.731	0.081	$>10^{39}$	∞	K_c, $\mathcal{D}_c$, $\mathcal{D}_y$, k_f
(g)	0.45	0.283	297	0.736	∞	∞	$>10^{39}$	K_c, $\mathcal{D}_c$, k_a
(h)	0.84	0.283	291	0.0076**	∞	∞	∞	K_c, $\mathcal{D}_c$
(i)	7.14	0.283	288	∞	∞	∞	∞	K_c

* Based on 151 equally spaced frequency values with termination at $|E(j\omega)| = 0.02$.
** This computation is based on an assumed uniform crystallite radius equal to the mean value, $\bar{R}_r = 3.14 \times 10^{-4}$ cm.

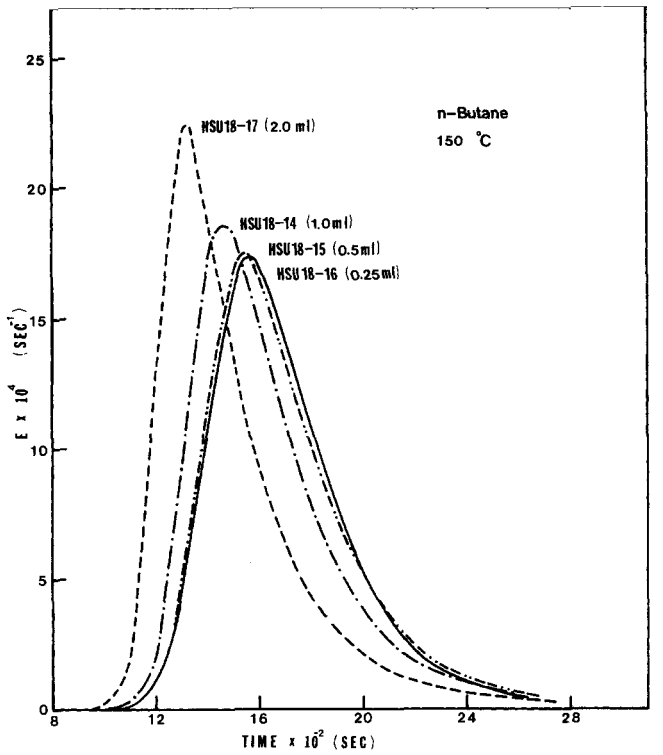

Figure 7. Linearity testing on the system n-butane/zeolite NaY at 150°C and 2.00 cm/s: Quantity in ( ) is pulse injection volume.

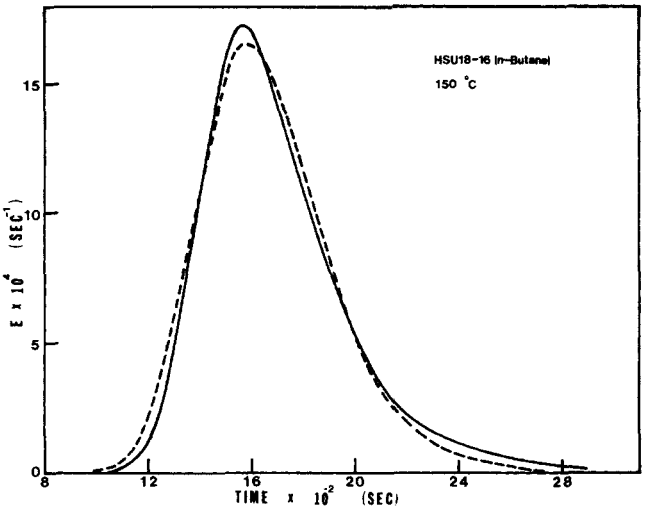

Figure 8. Comparison of "experimental" and calculated E-curves: solid curve, "experimental"; dashed curve is calculated ($\mathcal{D}_c = 0.545 \times 10^{-7}$ cm²/s, $K_c = 314$).

with the model.* An additional point of concern is provided by Figures 3 and 4. Curve (b) in these figures was calculated from the optimum parameter values (Table 2) and Eq. 31. There is a clear discrepancy between the calculated and experimental curves in these figures and in similar plots for all the results of Table 2.

Table 3 provides a sensitivity analysis on the results of Run HSU13-1. The objective function, ϕ, of Eq. 29 is tabulated for a number of computational experiments. Case (a) gave the optimized parameter set listed in Table 2. In cases (b) and (c), the axial dispersion coefficient was varied by ±20% to test the possibility that an error in the axial dispersion correlation might be responsible for the observed discrepancy. While some improvement in the fit (i.e., smaller ϕ) is indicated in case (b), this is hardly significant as can be judged from a comparison of the calculated and experimental curves in the time domain. A substantial reduction in ϕ is possible, if $\mathcal{D}_z$ is included in the optimization, case (d). However, the optimum value of $\mathcal{D}_z$ is unrealistic.

Although no evidence of a particle-size effect was indicated, we nevertheless included a macropore diffusion term in the analysis, case (e). No improvement in the objective function was found. Neither did provision for external mass transfer, case (f), nor finite rate of adsorption, case (g), result in any improvement in fit. It is really quite remarkable that the general six-parameter model cannot be made to fit the experimental data any better than the simplified three-parameter model.

It is noteworthy that the assumption of a constant average crystallite size, i.e. the model of Eqs. 13 and 23, results in a relatively poor fit to the data. (Compare cases (a) and (h) in Table 3.) Also note that the value of the diffusivity based on the mean particle size, $\bar{R}_p = 3.14 \times 10^{-4}$ cm, is about two orders of magnitude smaller than the true value. The fact that the optimization is sensitive to the crystallite-size distribution indicates that the crystallite diffusivity term is influencing the results. This is better illustrated by setting $\mathcal{D}_c = \infty$ and adjusting K_c alone to give the optimum fit case (i). The large increase in ϕ attests to the importance of the intracrystalline diffusion term. This is also illustrated in Figure 3 where the calculated response curve for $\mathcal{D}_c = \infty$ is plotted. At the higher temperature of Figure 4, the intracrystalline diffusion term is of less importance, but still significant.

Our failure to reconcile these discrepancies suggested the need for a more careful look at system linearity. In preliminary studies described by Hsu (1979), the concentration of butane in the sample valve was varied and the response curves appeared to be nearly independent of pulse concentration. However, these tests were conducted at relatively high temperatures where the diffusion contribution to the peak broadening is only moderate (T = 178°C) to low (T = 244°C).

Close examination of these results does indicate a small effect of pulse concentration, and it was decided to investigate this point further. The sample valve in Figure 1 was replaced with a sample injection port and dispersion column as described earlier. Different size pulses of n-butane were conveniently injected by means of a gas-tight syringe and both the input and output curves were recorded on a dual-pen recorder. The time domain E-curve was calculated by first transforming the experimental input, or X-curve, and output, or Y-curve, into the frequency domain and calculating $\bar{E}(j\omega)$ according to Eq. 27. The time domain E-curve was then calculated according to Eq. 31. Filon's method was employed in all the numerical integrations.

The results of a series of these linearity tests are plotted in Figure 7. Column conditions are the same in each of these experiments. Only the n-butane injection volume is varied. Clearly, the sample injection volume has a significant influence on the shape of the E-curve for sample volumes larger than about 0.25 mL. The system is nonlinear in this region and the linear chromatography theory would not be expected to apply. It is apparent that the differences between the E-curves for Runs HSU18-15 and HSU18-16 are not large, thus suggesting that the system may be approaching linearity for the smallest injection volume.

Unfortunately the output pulse was diluted to such an extent for injection volumes less than 0.25 mL that detector sensitivity became a problem and it was not possible to obtain reliable results in this region. Since Run HSU18-16 represented the closest approach to linearity in this series of experiments, the linear model was fit to this curve by adjusting the constants $\mathcal{D}_c$ and K_c. The corresponding E-curve was generated numerically and the results are plotted in Figure 8 for comparison with the experimental curve. The deviations between theory and experiment are very similar in both magnitude and trend to those

* Recently, Boersma-Klein and Moulijn (1979) calculated a similar velocity-dependent, effective diffusivity from their chromatography measurements. Their data were less extensive than ours and they attributed this variation to inaccuracies of measurements.

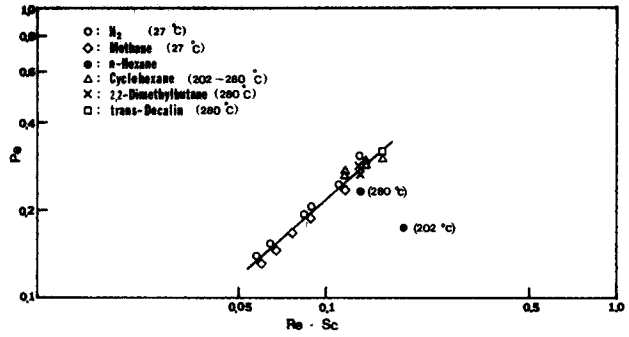

Figure 9. Axial dispersion correlation for Column No. 3.

found in experiments which utilized the sample injection valve. From the results in Figure 7, it appears that these small, but consistent, deviations are due to system nonlinearities.

Experiments with Other Hydrocarbons

Limited experiments were undertaken to evaluate the diffusivities of other hydrocarbon molecules in zeolite NaY. The apparatus was in the same configuration as just described; i.e., the sample injection port was used instead of the sample valve. Since the second column had been subjected to several temperature cycles, a third column was packed with fresh zeolite NaY. Details of column No. 3 are provided in Table 1.

As described earlier, a correlation for the axial dispersion coefficient was established from experiments with smaller molecular species. The plot of Pe vs. $Re \times Sc$ for column No. 3 is presented in Figure 9. Surprisingly, when the data for the large hydrocarbon species were treated in this fashion, all the points with the exception of the n-hexane data fell on a single curve. Furthermore, the E-curves in all except the n-hexane experiments were nearly symmetrical. No effect of pulse size was evident in experiments with cyclohexane and 2,2-dimethylbutane. (Pulse size was not varied in the *trans*-decalin experiment.)

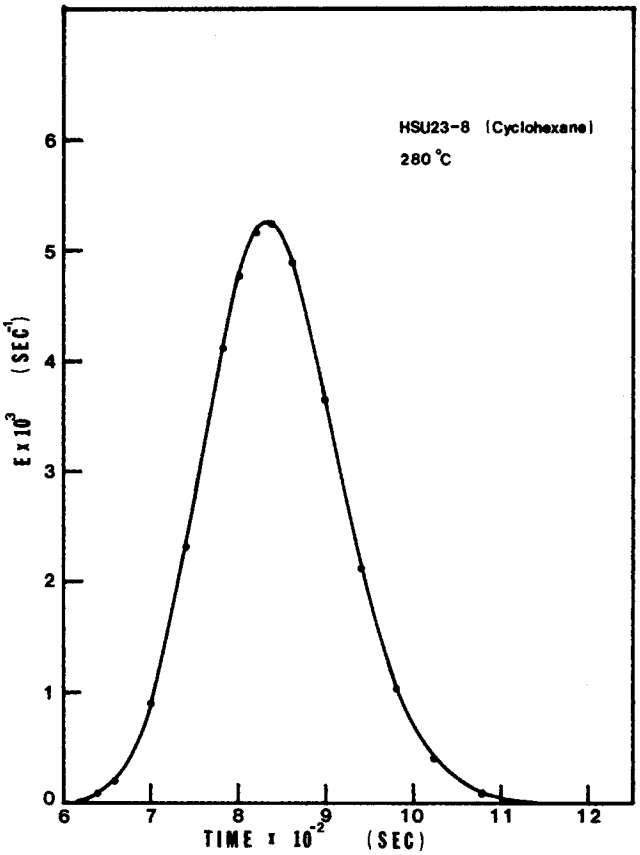

Figure 10. Comparison of "experimental" (solid line) and calculated (points) E-curves for cyclohexane/zeolite NaY experiment at 2.22 cm/s. Calculated curve for $\mathcal{D}_c = \infty$, $K_c = 174$, $\mathcal{D}_z = 0.281$ cm²/s.

The linear chromatography model provided a much better fit to the experimental results for cyclohexane, 2,2-dimethybutane and *trans*-decalin as compared with the n-butane results, Figures 10 to 12. In each of these figures, the calculate E-curves are for $\mathcal{D}_c = \infty$ and the optimization parameters were K_c and $\mathcal{D}_z$. Intracrystalline diffusion was too rapid to be detected in these systems over the range of temperatures studied: 202-280°C for

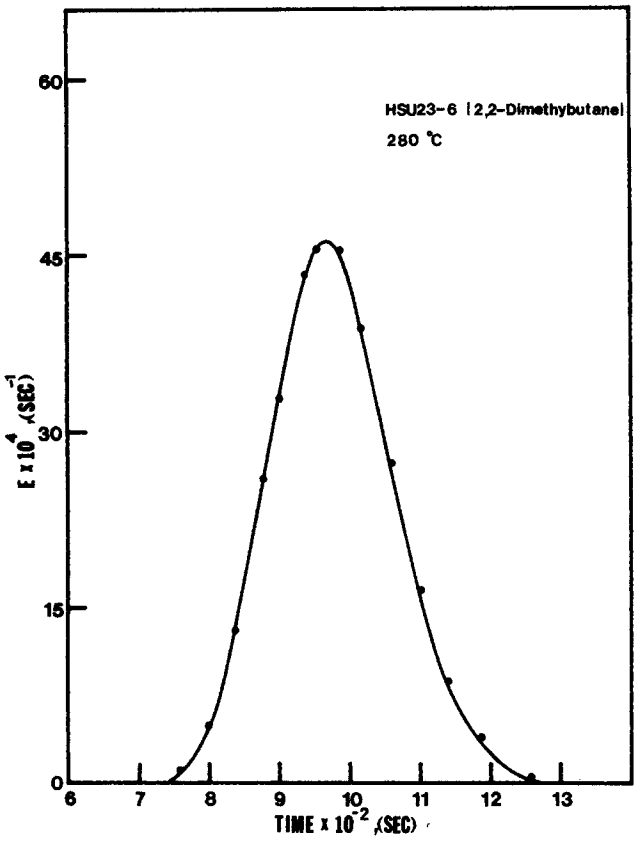

Figure 11. Comparison of "experimental" (solid line) and calculated (points) E-curves for 2,2-dimethylbutane/zeolite NaY experiment at 2.31 cm/s. Calculated curve for $\mathcal{D}_c = \infty$, $K_c = 211$, $\mathcal{D}_z = 0.282$ cm²/s.

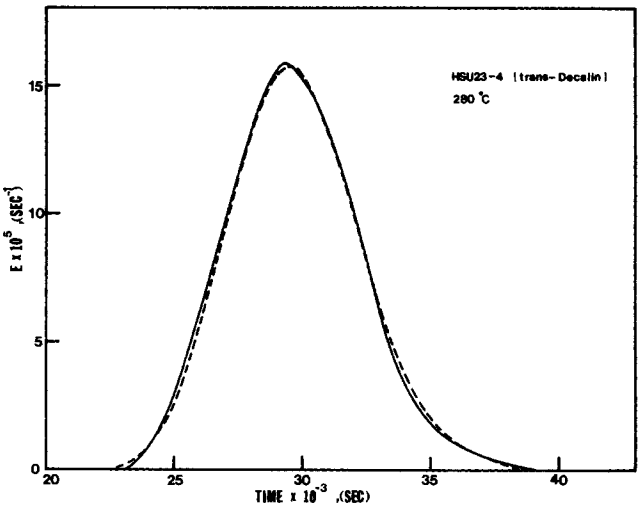

Figure 12. Comparison of "experimental" (solid line) and calculated (dashed line) E-curves for *trans*-decalin/zeolite NaY experiment at 2.38 cm/s. Calculated curve for $\mathcal{D}_c = \infty$, $K_c = 6670$, $\mathcal{D}_z = 0.268$ cm²/s.

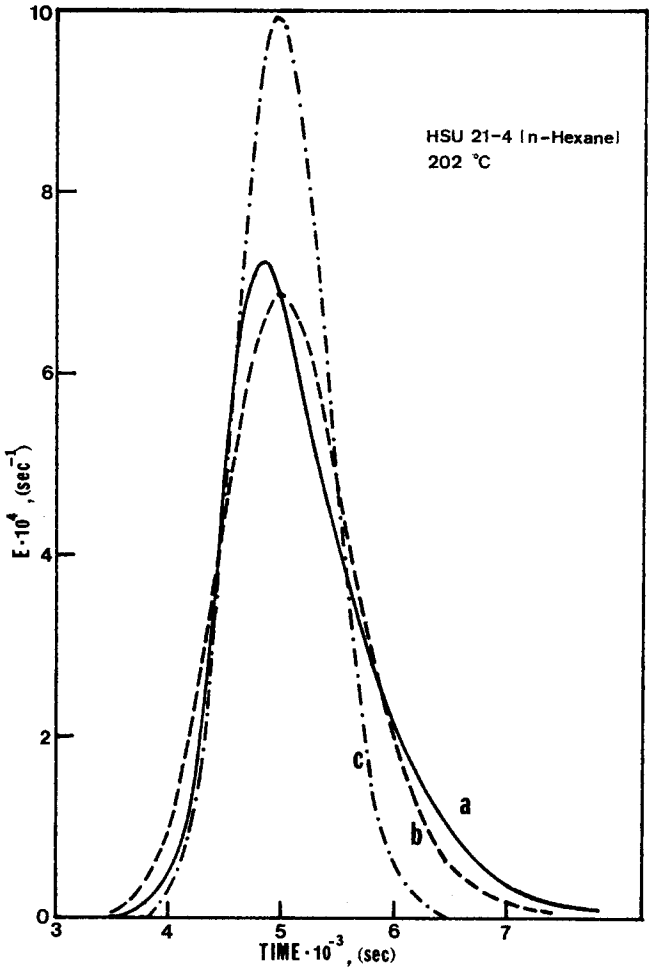

Figure 13. Comparison of "experimental" and calculated *E*-curves, for n-hexane diffusion in zeolite NaY at 202°C, 2.33 cm/s: *a* = experimental; *b* = calculated ($\mathcal{D}_c = 0.423 \times 10^{-7}$ cm²/s, $K_c = 1120$); *c* = calculated ($\mathcal{D}_c = \infty$, $K_c = 1100$).

cyclohexane, 280°C for 2,2-dimethylbutane and *trans*-decalin. For large hydrocarbon species, it is often impractical to conduct measurements at much lower temperatures because of the strong adsorption effect. Over 11 hours were required for elution of the *trans*-decalin peak for example, and detector sensitivity becomes a problem with such highly dispersed peaks.

The limited results from the n-hexane experiments were similar to the results obtained with n-butane. At 280°C, most of the pulse dispersion was due to axial dispersion; however, the contribution from intracrystalline diffusion was significant at 202°C. As illustrated in Figure 13 a discrepancy exists between the calculated and experimental response curves similar to the discrepancy observed with the n-butane results. Furthermore, a small effect of pulse size was observed. The calculated intracrystalline diffusivity of n-hexane in zeolite NaY, 0.423×10^{-7} cm²/s at 202°C, is about an order of magnitude smaller than the comparable n-butane value.

The temperature dependence of the adsorption constants is illustrated in Figure 5. Temperature was not varied in the experiments with 2,2-dimethybutane and *trans*-decalin. The sorption constant in Figure 5 is a modified Henry's law constant based on partial pressures rather than gas phase concentrations, and a conversion factor has been introduced to convert the adsorbed phase concentration from mol/cc to mol/cage. The heats of sorption derived from these plots should be considered low coverage values.

DISCUSSION

It is interesting to speculate on the source of the nonlinearities observed in the n-butane/NaY system. Three possibilities include: 1. non-Fickian diffusivity, 2. nonlinear sorption isotherm, and 3. nonisothermal sorption due to the heat effect. Single-particle heat transfer calculations assuming infinite rates of diffusion appear to rule out the heat effect, although the possibility of a localized heat effect has been suggested (Cerro and Smith, 1969). Cyclohexane sorption on NaY is more extensive and stronger than n-butane sorption, and yet the cyclohexane results are well described by the linear model. Thus, it seems unlikely that a heat effect is responsible for the n-butane nonlinearities.

Sorption on zeolites is normally consistent with the Langmuir isotherm, and only at low concentration levels is the sorption linear (Henry's law region). We have no means of ruling out possible nonlinear isotherm effects. But, it is noted that the nonlinearities in our system are only observed when intracrystalline diffusion is significant, i.e. for the experiments with n-butane and n-hexane. Ruthven and Doetsch (1976) found the Fickian diffusivities for several hydrocarbon species diffusing in zeolite NaX to be concentration-dependent even in the Henry's law region. Generally, according to Ruthven (1977), when the critical molecular diameter is small in comparison to the zeolite pore dimension, the Fickian diffusivity is inversely proportional to concentration; when the molecular dimensions and pore size are comparable, the Fickian diffusivity is constant.

The velocity dependence of the calculated n-butane diffusivities, Figure 6, is likely a consequence of system nonlinearities. As velocity increases (all other factors remaining constant), the pulse width decreases and the concentrations within the column increase giving rise to more pronounced nonlinearities. If this reasoning is correct, the low velocity runs should provide the most reasonable order of magnitude estimates of the intracrystalline diffusivities at infinite dilution.

We cannot conclude this discussion without mention of previous investigations of diffusion of n-butane and other hydrocarbons in faujasite-type zeolites. Unfortunately, the reported diffusivities are characterized by such great inconsistencies that a comparison of our approximate values with the literature values appears to have little meaning. This point is well illustrated by comparing the reported diffusivities of n-butane in zeolite NaX.

Lee and Ma (1977) obtained diffusivity values of the order of 10^{-14} to 10^{-13} cm²/s over a range of temperatures from 5 to 60°C using a technique involving unsteady-state sorption in a constant volume chamber. When extrapolated to the same temperature range as employed in our study, Lee and Ma's diffusivities are some four orders of magnitude smaller than our values. Doelle and Riekert (1977) using a gravimetric sorption technique found the diffusivity of n-butane in zeolite NaX to be of the order of 10^{-7} cm²/s at 25°C. This value is two to three orders of magnitude greater than the results of our study would indicate. Still larger values of diffusivity are obtained by the NMR pulsed field gradient technique. Karger et al. (1975) reported n-butane diffusivities of the order of 10^{-5} cm²/s in zeolite NaX at 20°C.

The reasons for these inconsistencies are unclear at the present time, although in some cases probable explanations have been set forth. There is evidence, for example, that a thermal effect may cloud the results of adsorption rate determinations in static systems (Doelle and Riekert, 1977; Lee and Ruthven, 1978; Chihara et al., 1976). In the present investigation we have shown that the common usage of an average particle size in the calculations can result in an error of two orders of magnitude in the reported diffusivity. One of the problems in evaluating the intracrystalline diffusivity is that the techniques employed are generally responsive to factors other than the intracrystalline diffusivity. Evaluation of the intracrystalline diffusivity, therefore, requires a precise model and meticulous attention must be paid to the data analysis.

ACKNOWLEDGMENTS

Financial support for this project was provided by the U.S. Department of Energy under contract No. DE-AS22-77ET10651. We also wish to acknowledge the assistance of M. P. Mathur of U.S.D.O.E./P.E.T.C. who kindly provided the crystallite size analysis.

NOTATION

C = gas phase concentration of diffusion species, mol/cc
$\mathcal{D}$ = diffusion or dispersion coefficient based on total area, cm^2/s
E = residence time distribution function (normalized response curve), s^{-1}
Im = imaginary part of transformed pulse
K_a = crystallite adsorption equilibrium constant (two-phase adsorption model)
K_c = crystallite sorption equilibrium constant
K_v = macropore adsorption equilibrium constant
k_a = adsorption rate constant, cm/s
k_f = external mass transfer coefficient, cm/s
L = column length, cm
$p(R_x)$ = crystal size distribution function
q = sorbed phase concentration, mol adsorbate/cc crystal
R = particle radius, cm
Re = real part of transformed pulse
s = Laplace transform variable
t = time, s
v = superficial velocity, cm/s
$\mathcal{W}$ = rate at which diffusing component leaves particle or crystallite, mol/cc · s
X = input curve, arbitrary concentration units
x = radial distance from center of crystallite, cm
Y = output (response) curve, arbitrary concentration units
y = radial distance from center of pellet, cm
z = axial distance from column entrance, cm; or, dummy variable of integration, Eq. 22

Greek Letters

ϕ' = objective function, Eq. 28
ϕ = objective function, Eq. 29
θ_x = micropore porosity (two-phase adsorption model), cc micropore/cc crystallite
θ_y = macropore porosity, cc macropore/cc pellet
θ_z = column porosity, cc bed voids/cc bed
γ = quantity defined by Eq. 14
β = quantity defined by Eq. 15
α = quantity defined by Eq. 16
σ = parameter in crystal size distribution function, Eq. 20
μ = parameter in crystal size distribution function, Eq. 20
ω = frequency, s^{-1}

Subscripts

c = crystallite quantity or calculated quantity
m = molecular quantity
x = microparticle (crystallite) quantity
y = pellet quantity
z = column quantity

LITERATURE CITED

Boersma-Klein, W., and J. A. Moulijn, "The Evaluation in Time Domain of Mass Transfer Parameters From Chromatographic Peaks," *Chem. Eng. Sci.*, **34**, 959 (1979).

Cerro, R. L., and J. M. Smith, "Effects of Heat Release and Nonlinear Equilibrium on Transient Adsorption," *Ind. Eng. Chem., Fund.*, **8**, 796 (1969).

Chihara, K., M. Suzuki, and K. Kawazoe, "Effect of Heat Generation on Measurement of Adsorption by Gravimetric Method," *Chem. Eng. Sci.*, **31**, 505 (1976).

Chou, T. S., "Design of a Pulse Diffusivity Apparatus for Improved Sensitivity," *Chem. Eng. Sci.*, **34**, 133 (1979).

Doelle, H. J., and L. Riekert, "Kinetics of Sorption, Desorption, and Diffusion of n-Butane in Zeolite NaX," *ACS Symp. Ser.*, **40**, 401 (1977).

Edwards, M. F., and J. F. Richardson, "Gas Dispersion in Packed Beds," *Chem. Eng. Sci.*, **23**, 109 (1968).

Gangwal, S. K., R. R. Hudgins, and P. L. Silveston, "Conditions Needed for Satisfactory Measurement of Mass Transfer Coefficients, Internal Diffusivity and Adsorption Rate Constants," *Can. J. Chem. Engr.*, **56**, 554 (1978).

Gunn, D. J., "Theory of Axial and Radial Dispersion in Peaked Beds," *Trans. Instn. Chem. Engrs.*, **47**, T351 (1969).

Hashimoto, N., and J. M. Smith, "Macropore Diffusion in Molecular Sieve Pellets by Chromatography," *Ind. Eng. Chem. Fund.*, **12**, 353 (1973).

Haynes, Jr., H. W., "Chemical, Physical, and Catalytic Properties of Large Pore Acidic Zeolites," *Catal. Rev.—Sci. Eng.*, **17**, 273 (1978).

Haynes, Jr., H. W., "The Determination of Effective Diffusion by Gas Chromatography. Time Domain Solutions," *Chem. Eng. Sci.*, **30**, 955 (1975).

Haynes, Jr., H. W., and P. N. Sarma, "A Model for the Application of Gas Chromatography to Measurements of Diffusion in Bidisperse Structured Catalysts," *A.I.Ch.E. J.*, **19**, 1043 (1973).

Hays, J. R., W. C. Clements, Jr., and T. R. Harris, "The Frequency Domain Evaluation of Mathematical Models for Dynamic Systems," *A.I.Ch.E. J.*, **13**, 374 (1967).

Hsiang, T. C. S., and H. W. Haynes, Jr., "Axial Dispersion in Small Diameter Beds of Large, Spherical Particles," *Chem. Eng. Sci.*, **32**, 678 (1977).

Hsu, L. K. P., "Effective Diffusivities by the Gas Chromatography Technique. Studies on the System n-Butane/Zeolite NaY," M.S. Thesis, Univ. of Mississippi (1979).

Karger, J., S. P. Shdanov, and A. Walter, "NMR-Untersuchungen Zur intrakristallinen Selbstdiffusion von n-Butan und n-Heptan an NaX-Zeolithen," *Z. Phys. Chem. (Leipsig)*, **256**, 319 (1975).

Lee, L. K., and D. M. Ruthven, "Analysis of Thermal Effects in Adsorption Rate Measurements," *J. Chem. Soc., Faraday Trans. I.*, **75**, 2406 (1979).

Lee, T. Y., and Y. H. Ma, "Effects of Exchangeable Cations on Diffusion in Faujasite Pellets," *ACS Symp. Ser.*, **40**, 428 (1977).

Miyauchi, T., and T. Kikuchi, "Axial Dispersion in Packed Beds," *Chem. Eng. Sci.*, **30**, 343 (1975).

Ruthven, D. M., "Diffusion in Molecular Sieves: A Review of Recent Developments," *ACS Symp. Ser.*, **40**, 320 (1977).

Ruthven, D. M., and I. H. Doetsch, "Diffusion of Hydrocarbons in 13X Zeolite," *A.I.Ch.E. J.*, **22**, 822 (1976).

Sarma, P. N., and H. W. Haynes, Jr., "Application of Gas Chromatography to Measurements of Diffusion in Zeolites," *Adv. Chem. Ser.*, **133**, 205 (1974).

Sarma, P. N., and H. W. Haynes, Jr., "Effective Macropore Diffusivity of Bidisperse Structured Catalysts by Gas Chromatography," paper 65g, 67th Ann. Mtg. of AIChE, Washington (1974b).

Satterfield, C. N., *Mass Transfer in Heterogenous Catalysis*, M.I.T. Press, Cambridge, Mass. (1970).

Scheid, F., *Theory and Problems of Numerical Analysis* (Schaum's Outline Series), McGraw-Hill, New York (1968).

Shah, D. B., and D. M. Ruthven, "Measurement of Zeolitic Diffusivities and Equilibrium Isotherms by Chromatography," *A.I.Ch.E. J.*, **23**, 804 (1977).

Suzuki, M., and J. M. Smith, "Axial Dispersion in Beds of Small Particles," *Chem. Eng. J.*, **3**, 256 (1972).

Tranter, C. J., *Integral Transforms in Mathematical Physics*, Chapman and Hall, London (1971).

Wakao, N., S. Kaguei, and T. Funazkri, "Effect of Fluid Dispersion Coefficients on Particle-to-Fluid Heat Transfer Coefficients in Packed Beds," *Chem. Eng. Sci.*, **34**, 325 (1979).

Wakao, N., K. Tanaka, H. Nagai, "Measurements of Particle-to-Gas Mass Transfer Coefficients from Chromatographic Adsorption Experiments," *Chem. Eng. Sci.*, **31**, 1109 (1976).

Manuscript received December 3, 1979; revision received April 22, and accepted May 7, 1980.